V-D Magnetic Structure of Oligo-Nitroxide-Transition Metal Complexes

Since one or two decades, considerable attention has been devoted to stable nitroxide radicals and their metal complexes which are now widely used as building blockes for the design of moleculaer-based magnetic materials. In this field, we have introduced a new strategy of employing π-conjugated polyaminoxyls as ligands in which the 2*p*-spins of the NO groups interact ferromagnetically ($J_1 > 0$). The dimensionality of the complex and the sign and magnitude of the exchange coupling between the neighboring spins may be readily tuned by this strategy. Depending on the nature of the additional interchain or interlayer interaction, the polymers are expected to become an antiferromagnet or ferri/ferromagnet. By modifying and extending this design strategy to bis- and tris(aminoxyl) radicals having triplet and quartet ground states, respectively, we have been able to construct with the aid of magnetic metal ions one-dimensional (1D) chain, two-dimensional (2D) network and three-dimensional (3D) parallel-crosses structures in which both the organic 2p and metallic 3d spins have been ordered in macroscopic scales. Since such a rational approach by self-assembly to the tailored extended systems having relevant physical properties is of great importance in materials synthesis. For these materials, the magnetic structures of the crystals are also interesting.

V-D-1 Influence of the Thermal Excitations of the Ferrimagnetic (–1/2,5/2,–1/2) Linear Trimer on the Paramagnetic Behavior of the Layered Metal-Radical Complex $\{Mn(hfac)_2\}_3(R_X)_2 \cdot n\text{-}C_7H_{16}$

MARKOSYAN, Ashot S.[1]; **HOSOKOSHI, Yuko; INOUE, Katsuya**
([1]*IMS and Moscow State Univ., Russia)*

[*Phys. Lett. A* **261**, 212 (1999)]

The complex $\{Mn(hfac)_2\}_3(\mathbf{3R}_\Delta)_2 \cdot n\text{-}C_7H_{16}$ forms a two-dimensional honeycomb-like spin network. It is shown that the spins of Mn(II) form with the two 1/2-spins of different adjacent triradicals $\mathbf{3R}_\Delta$ linear $(\bar{1}/2,5/2,\bar{1}/2)$ ferrimagnetic trimers, which determine the paramagnetic properties of the complex. The intratrimer excitations result in the decay of the trimers above 140 K. The experimental data can well be described within this model both at high and low temperatures thus proving the importance of the thermal excitations within the trimers. The best agreement was obtained at J_{TR}/k = –176.4 K and λ' = +0.333 emu/mol. The power series expansion for the 2D honeycomb network gives J_{TR}/k = –175.4 K and J_1/k = +0.226 K.

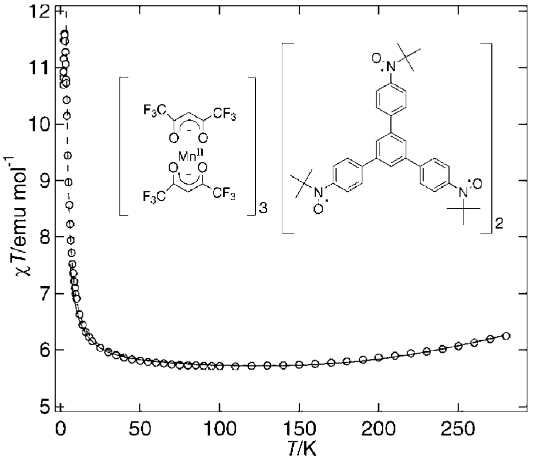

Figure 1. The temperature dependence of $\chi_m T$ for the layered complex $\{Mn(hfac)_2\}_3(\mathbf{3R}_\Delta)_2 \cdot n\text{-}C_7H_{16}$. Open circles are the experimental data, the solid and the dashed lines are the least squares fits for a 2D and 3D lattice, respectively.

V-D-2 Synthesis and Magnetic Properties of Bis(hexafluoroacetylacetonate) Copper(II) Complex with 5-Bromo-1,3-Phenylenebis(*N-tert*-butylaminoxyl) as a Bridging Ligand

IWAHORI, Fumiyasu; INOUE, Katsuya; IWAMURA, Hiizu[1]
([1]*Kyushu Univ.)*

[*Mol. Cryst. Liq. Cryst.* **334**, 533 (1999)]

Bis(hexafluoroacetylacetonato)copper(II), $Cu(hfac)_2$ (= M) reacts with 5-bromo-1,3-phenylenebis(*N-tert*-butylaminoxyl), $\mathbf{1}_{Br}$ to yield a complex of formula $[M_3 \cdot (\mathbf{1}_{Br})_2]$. The X-ray crystal structure shows that it crystallize in the space group *P*1, with *a* = 12.469(2) Å, *b* = 15.278(2) Å, *c* = 11.602(2) Å, α = 104.59(1)°, β = 111.86(1)°, γ = 88.32(1)°, and *Z* = 1. The crystal contains copper(II) trinuclear structure, M-$\mathbf{1}_{Br}$-M-$\mathbf{1}_{Br}$-M. The magnetic susceptibility measurements revealed a structual transition at *ca.* 48 K accompanied by a temperature hysterisis. (Figure 1)

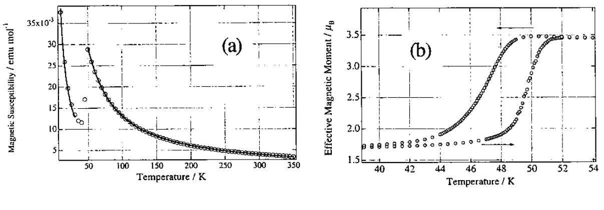

Figure 1. (a) χ_m versus *T* plot for $[Cu(hfac)_2]_3(\mathbf{1}_{Br})_2$ measured at a magnetic field of 50000 Oe; (b) Observed μ_{eff} versus *T* plots in the temperature range 39–45 K. Solid lines are calculated on Curie-Weiss law (15–45 K) and the trinuclear complex model (50–350 K).

V-D-3 Magnetic Behaviour of the Ferrimagnetic (–1/2,5/2,–1/2) Linear Trimer in Complexes of $Mn(hfac)_2$ with Bis- and Trisnitroxide Radicals

MARKOSYAN, Ashot S.[1]; **IWAMURA, Hiizu**[2]; **INOUE, Katsuya**
([1]*IMS and Moscow State Univ., Russia;* [2]*Kyushu Univ.)*

[*Mol. Cryst. Liq. Cryst.* **334**, 549 (1999)]

Characterization and magnetic properties of new metal-radical complexes with bivalent Mn having a general formula $\{[\mathrm{Mn(hfac)_2}]_m(\mathbf{R})_n\}$ are given. (Figure 1) In these complexes, the aminoxyl radicals have magnetic, triplet or qualtet, ground state and form with Mn^{2+} heterospin structures. They show 1D, 2D, and 3D behaviour depending on the crystal structure, chemical formula and molecular structure of radical. In the ordered state, the complexes form a ferrimagnetic structure due to a strong nagetive coupling between the radical and Mn spins. Magnetic anisotropy in some single crystal was studied. The 3D complex $\{[\mathrm{Mn(hfac)_2}]_3(\mathbf{3R}_\mathrm{T})_2\}$ with a linear triradical can be described within a sublattice model of ferrimagnetism, one sublattice of which os formed by 1D chains, while the other consists of magnetically isolated Mn^{2+} ions. Its comparatively high T_C = 45 K is accounted for the large interchain exchange interaction (3.9 K) through the isolated Mn^{2+}.

Analysis of their paramagnetic properties shows that the hagher energy excitations are related to the desintegration of the ferrimagnetic (–1/2,5/2,–1/2) linear trimer species, which can be isolated in all these compounds.

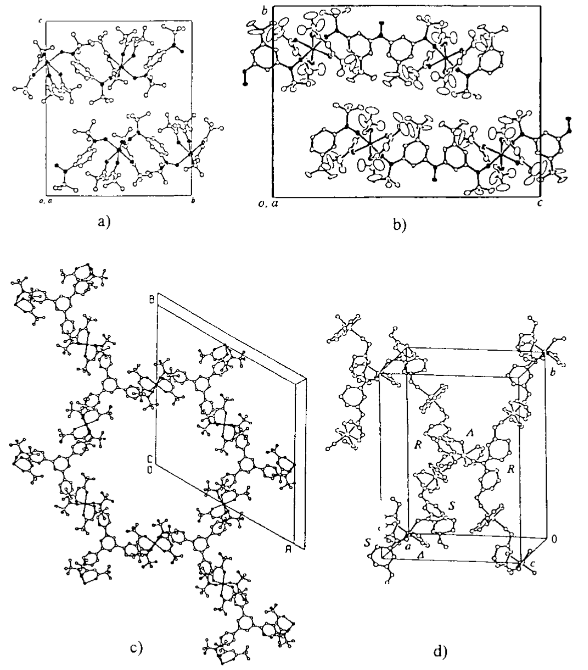

a) b)

c) d)

Figure 1. 1D chains of $\{[\mathrm{Mn(hfac)_2}](\mathbf{2R})\}$ extending along *b*-axis (a); an enatiomeric pair of isotactic 1D chains of $\{[\mathrm{Mn(hfac)_2}](\mathbf{3R}_\mathrm{T})\cdot n\text{-}\mathrm{C_6H_{14}}\}$ (the molecules of $n\text{-}\mathrm{C_6H_{14}}$ are disordered and not shown for clarity) (b); 2D hexagonal net of $\{[\mathrm{Mn(hfac)_2}]_3(\mathbf{3R}_\Delta)_2\cdot n\text{-}\mathrm{C_7H_{16}}\}$ viewed down to the *c*-axis (the $n\text{-}\mathrm{C_7H_{16}}$ molecules are not shown) (d); 3D parallel-crossed structure of $\{[\mathrm{Mn(hfac)_2}]_3(\mathbf{3R}_\mathrm{T})_2\}$ (the $\mathrm{CF_3}$ and $\mathrm{(CH_3)_2C}$ groups are not shown.

V-D-4 Exchange Coupling Parameters and Energy Levels for Cyclic Metal-Radical Complexes of Bis(hexafluoroacetylacetonato) manganese(II) with 5-*tert*-butyl-1,3-phenylenebis(*N*-*tert*-butyl-aminoxyl) and (4-*N*-*tert*-butyl-*N*-oxyamino)pyridine

RABU, Pierre[1]; DRILLON, Marc[1]; IWAMURA, Hiizu[2]; GÖITZ, Gunter[2]; ITOH, Tetsuji[2]; MATSUDA, Kenji[2]; KOGA, Noboru[2]; INOUE, Katsuya
([1]Inst. Phys. Chim. Matér. Strasbourg, France; [2]Kyushu Univ.)

[*Eur. J. Inorg. Chem.* **211**, 216 (2000)]

Temperature-dependant paramagnetic susceptibility data for two cyclic dimer complexes of bis(hexafluoroacetylacetonato)manganese (II) with 5-*tert*-butyl-1,3-phenylenebis(*N*-*tert*-butylaminoxyl) **1** and 4-(*N*-*tert*-butyl-*N*-oxyamino)pyridine have been analyzed to obtain two sets of two intermolecular exchange coupling parameters J_1 and J_2. (Figure 1, Scheme 1) A previous model, based on one of these interractions being much weaker than the other, could not be explicitly correlated to these actual exchange-coupling paramaters. However, the energy levels of the low lying spin states were found to be reproduced reasonably well by the approximate method.

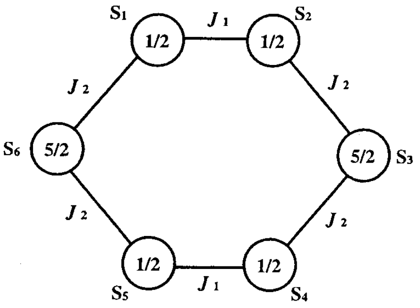

Scheme 1. A cyclic arrangement of the spins in $[\mathrm{Mn(hfac)_2}\cdot\mathbf{1}]_2$.

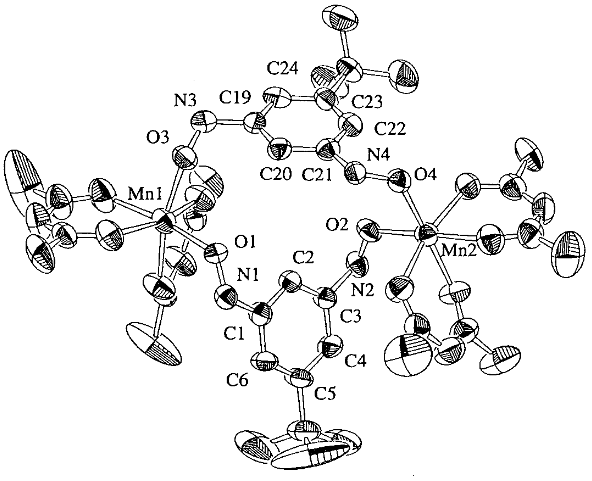

Figure 1. Structure of the cyclic complex $[\mathrm{Mn(hfac)_2}\cdot\mathbf{1}]_2$; Fluorine atoms, *N*-*tert*-Butyl groups and hydrogene atoms are omitted for clarity; thermal ellipsoids are drawn at the 50% probability level.

V-D-5 Synthesis and Magnetic Properties of a New Complex Made up of $\mathrm{Mn(hfac)_2}$ and a Radical with a Triplet Ground State

KUMAGAI, Hitoshi; HOSOKOSHI, Yuko; MARKOSYAN, Ashot S.[1]; INOUE, Katsuya

([1]IMS and M.V. Lomonosov Moscow State Univ.)

[*New J. Chem.* **24**, 537 (2000)]

A new metal-radical complex of Mn(II) made up of Mn(hfac)$_2$ and the radical 4-*N*-*tert*-butylaminoxyl-4'-(1-oxyl-3-oxide-4,4,5,5-tetramethylimidazolin-2-yl)-biphenyl (BIPNNNO) was synthesized. The X-ray single crystal structural analysis revealed that the complex consists of discrete molecules [Mn(hfac)$_2$]·(BIPNNNO)$_2$. The magnetic characteristics of this complex were studied and the Mn–radical and intraradical exchange integrals were evaluated: –135 ± 10 K and 72 ± 5 K, respectively. These values are compared with those of complexes of Mn(hfac)$_2$ with different aminoxyl polyradicals.

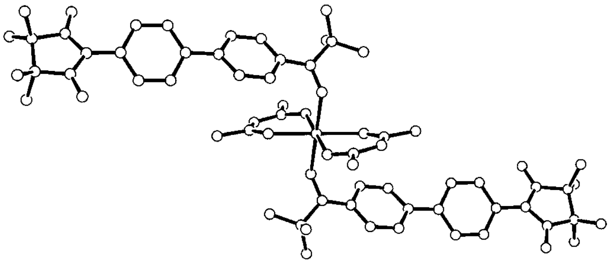

Figure 1. View of the discrete structure of Mn(hfac)$_2$-(BIPNNNO)$_2$.

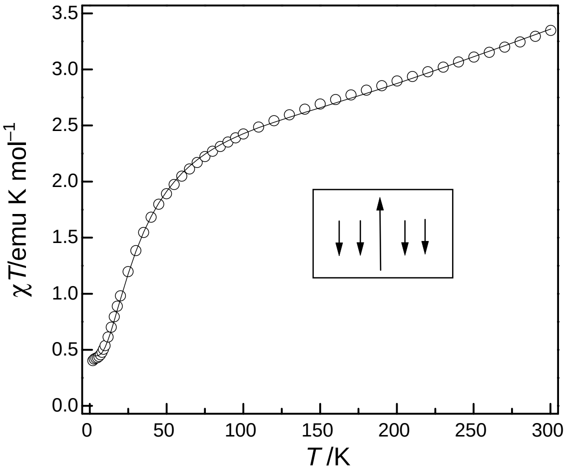

Figure 2. Temperature dependence of χ_mT of the complex Mn(hfac)$_2$(BIPNNNO)$_2$. The experimental data are shown by symbols and the solid line is the theoretical fit. The spin scheme of the complex is drawn in the frame.

V-D-6 Two-Dimensional Complexes of the General Formula [Mn(hfac)$_2$]$_3$·(R)$_2$ with Variable Metal-Radical Exchange Interactions

TANAKA AKITA, Motoko; HOSOKOSHI, Yuko; MARKOSYAN, Ashot S.[1]; IWAMURA, Hiizu[2]; INOUE, Katsuya

([1]IMS and M.V. Lomonosov Moscow State Univ.; [2]Kyushu Univ)

[*J. Phys. Chem.* submitted]

Magnetic properties of a series of new layered metal-nitroxide polyradical complexes with the general formula [M(hfac)$_2$]$_3$($\mathbf{R}_\Delta$)$_2$, M = Mn(II) or Cu(II), are studied. In these complexes the radicals have a quartet ground state and contribute essentially in magnetism. Several exchange interactions, between M and the NO group of the radical, the intraradical NO–NO interactions, are responsible in forming the magnetic properties of these heterospin systems. Depending on the character of the interlayer chemical bonds, they show either ferro/ferrimagnetic or antiferromagnetic long range order. The hirerachry of the different exchange interactions is established and the Mn–NO and Cu–NO exchange integrals are evaluated from analysis of the temperature dependence of the paramagnetic susceptibility. With increasing intraradical exchange interaction, the complexes exhibit a clear 2D behavior.

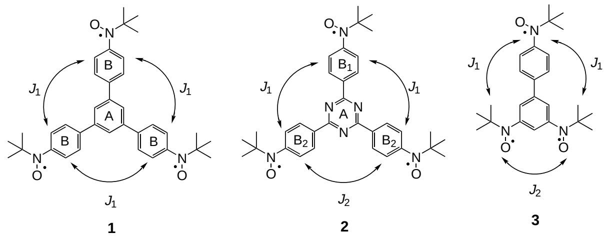

Figure 1. Triangular triradicals **1**, **2** and **3** with three ligating sites. A and B indicate the aromatic rings in different positions.

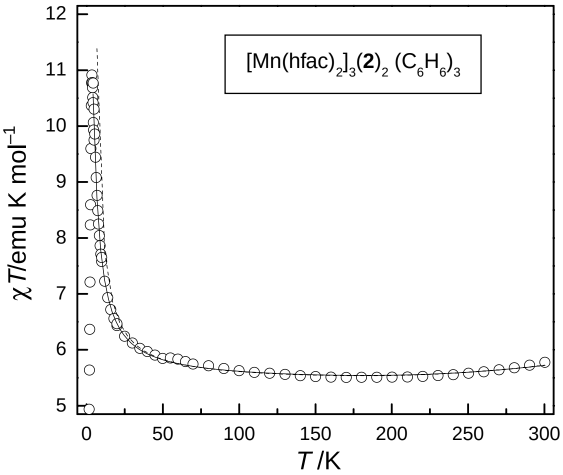

Figure 2. The temperature dependence of the product χ_mT for the complex [Mn(hfac)$_2$]$_3$(**2**)$_2$·(C$_6$H$_6$)$_3$. Open circles are the experimental data. The solid and the dot lines are the theoretical fits in the 2D and 3D models, respectively.

V-E Synthesis of Chiral Molecule-Based Magnets

The design of molecular materials with interesting magnetic and optical or electrical properties is one of the major challenges in the last few years. The synthesis and study of chiral molecular-based magnetic materials which are transparent for light are of great interest. Novel magneto-optical phenomena have been theoretically predicted and observed in chiral paramagnetic materials in 1997. Although novel properties are expected for such compounds, few examples of chiral molecular-based magnetic materials are still known. To get more insight in their properties it is therefore important to construct such chiral molecule-based magnets in a systematic way. We designed and synthesized a chiral organic radical which was can be employed to construct chiral molecular-based magnets.

V-E-1 Synthesis and Characterization of a Chiral Molecule-Based Metamagnet Made by a Chiral Triplet Organic Radical and Transition Metal Ion

KUMAGAI, Hitoshi; INOUE, Katsuya

[*Mol. Cryst. Liq. Cryst.* **334**, 487 (1999)]

Crystals of $\{\mathbf{1}\cdot\mathrm{M(II)(hfac)_2}\}_n$ (M = Mn, Cu) were obtained by mixing the 1,3-bis(*N*-*tert*-butylamino-*N*-oxyl)-5-{1-methyl-1-((*S*)-2-methylbutoxy)ethyl}-benzene (**1**) and bis(hexafluoroacetylacetonato)M(II) {M(II)·(hfac)$_2$} in diethyl ether/*n*-heptane. A single crystal of $\{\mathbf{1}\cdot\mathrm{Mn(II)(hfac)_2}\}_n$ is triclinic, space group $P1$ (No. 1), with a = 11.0005(3) Å, b = 11.8183(4) Å, c = 17.7135(7) Å, α = 81.607(3)°, β = 84.801(3)°, γ = 63.516(2)°, V = 2038.3(1) Å^3, and D_X = 1.380 g/cm^3 for Z = 1. A single crystal of $\{\mathbf{1}\cdot\mathrm{Cu(II)(hfac)_2}\}_n$ is triclinic, space group $P1$ (No. 1), with a = 11.2831(7) Å, b = 11.5615(7) Å, c = 18.0163(9) Å, α = 82.384(4)°, β = 74.242(4)°, γ = 61.826(5)°, V = 1993.9(2) Å^3, and D_X = 1.43 g/cm^3 for Z = 1. An X-ray crystal structure analysis revealed the formation of a helical one-dimensional polymeric structure. It not only contains a (*S*) chiral carbon center but also (*R*) C2 chiral skeleton of the 1,3-bis(*N*-*tert*-butylamino-*N*-oxyl)benzene moiety. Each of the two aminoxyl radical centers are coupled ferromagnetically within the organic radical molecule and is coupled antiferromagnetically to the d^5 manganese(II) ions. The temperature dependence of the magnetization revealed that the heterospin system behaves as a metamagnet below 5.4 K. (Figure 1)

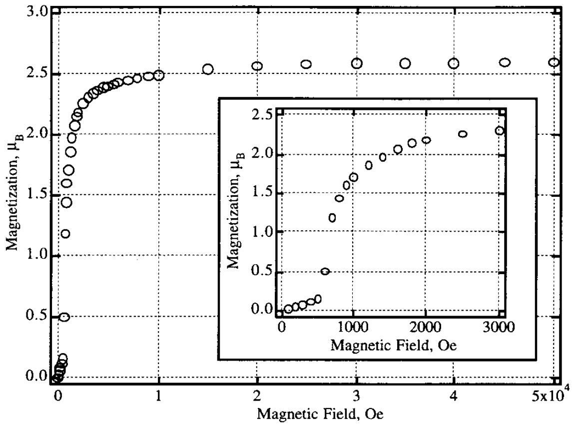

Figure 1. Field dependence of the magnetic moment at 1.8 K. Inset shows magnetic field range of 0 to 3000 Oe.

V-E-2 Synthesis, Structure and Magnetic Properties of a Chiral One-Dimensional Molecule-Based Magnet

KUMAGAI, Hitoshi; MARKOSYAN, Ashot S.[1]; INOUE, Katsuya
([1]IMS and Moscow State Univ., Russia)

[*Mol. Cryst. Liq. Cryst.* **343**, 97 (2000)]

A novel chiral organic radical 2-{4'-((*S*)-2''-methylbutoxy)phenyl}-4,4,5,5-tetramethylimidazoline-1-oxyl-3-oxide (**1**) and its metal complex, $[\mathbf{1}\cdot\mathrm{Mn(II)(hfac)_2}]_n$ were synthesized and characterized. The radical **1** crystallizes in the orthorhombic space group $P2_12_12_1$ (No. 19) with a = 11.494(3) Å, b = 25.328(3) Å, c = 6.1281(5) Å, V = 1748.0(4) Å^3. The complex $[\mathbf{1}\cdot\mathrm{Mn(II)(hfac)_2}]_n$ crystallizes in the same space group with a = 14.081(1) Å, b = 15.940(1) Å, c = 16.075(1) Å, V = 3608.1(4) Å^3. X-ray crystal structure analysis of the complex revealed the formation of a helical-chain structure. (Figure 1) The oxygen atoms of the radical **1** are ligated to two different manganese ions in cis position and exhibit the Δ configuration in $[\mathbf{1}\cdot\mathrm{Mn(II)(hfac)_2}]_n$. The magnetic measurements revealed that this chiral complex behaves as a ferrimagnet below T_C = 4.5 K. It is characterized by a strong intrachain exchange correlation, the ratio between the intrachain and interchain exchange interactions being about 10^{-5}.

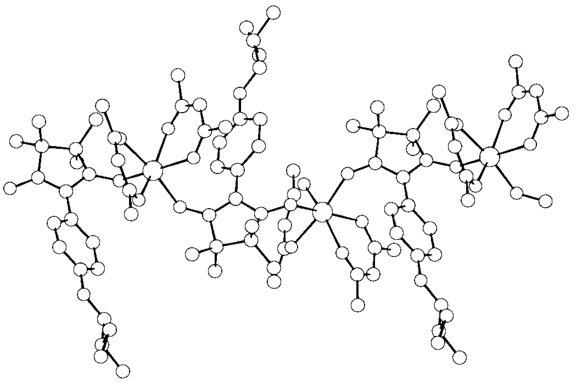

Figure 1. The X-ray crystal structure of the complex of $[\mathbf{1}\cdot\mathrm{Mn(II)(hfac)_2}]_n$. Hydrogene atoms and fluorine atoms are omitted for clarity.

V-F Synthesis and Characterization of Quantum-Spin Systems

There has been considerable current interest in the study of a low-dimensional quantum-spin system with an energy gap. Organic radicals suit such study, since they consist only of light elements and form ideal Heisenberg spin systems. By the appropriate design of molecules, we can obtain a variety of Heisenberg spin systems. As S = 1/2 antiferromagnetic lattices, we have synthesized a frustrated double chain system with an energy gap. Moreover, we have developed the study of intermediate state between S = 1/2 and S = 1. We have synthesized novel S = 1 species made of organic biradicals, having strong intramolecular exchange couplings of $2J/k_B$ ~ 200–700 K ($H = -2J\boldsymbol{S}_i \cdot \boldsymbol{S}_j$). Connection of the S = 1 molecules by the intermolecular antiferromagnetic exchange couplings in the crystalline state, leads to the intermediate state between S = 1/2 and S = 1. Adding to these, we focus on the ladder system, which is interesting in terms of Haldane state and the high T_C superconductivity. For the S = 1/2 Heisenberg spin ladder with antiferromagnetic legs and rungs, the ground state of the resonating valence bond (RVB) state or the dimerized state is theoretically expected. Experimentally, the singlet ground state was observed in some ladder systems formed by Cu-based compounds. The study of spin ladder systems has been mainly devoted to that of S = 1/2, but that of S = 1 is also interesting. For the ground state of the S = 1 ladder with antiferromagnetic legs ($J_\parallel$) and rungs ($J_\perp$), the Haldane state is expected in the extreme limit of $J_\perp \to 0$, and the dimer state in $J_\parallel \to 0$. In its ground state phase diagram on the $J_\parallel / J_\perp$ versus the energy gap (Δ), the phase transition from the dimer state to the Haldane state through a gapless point can be expected. A similar behavior of an existence of a gapless point between two different phases with their own finite excitation gaps is known for the S = 1 Heisenberg alternating antiferromagnetic chain system.

V-F-1 Construction of a Quantum-Spin System of S = 1/2 Antiferromagnetic Chain with the Next-Nearest-Neighbor Interactions

HOSOKOSHI, Yuko; KATOH, Keiichi; INOUE, Katsuya; GOTO, Tsuneaki[1]
([1]ISSP, Univ. Tokyo)

[*J. Phys. Soc. Jpn.* **68**, 2910 (1999)]

We have succeeded in synthesizing a new compound of a railroad trestle model, *i.e.*, a zigzag chain with next-nearest-neighbor interactions, having energy gap above the singlet ground state. We have synthesized novel organic radicals F_2PIMNH and Cl_2PIMNH, where F_2PIMNH = 2-[4'-*N*-*tert*-butylamino-2',6'-difluorophenyl]-4,4,5,5-tetramethyl-4,5-dihydro-1*H*-imidazol-1-oxyl and Cl_2PIMNH = 2-[4'-*N*-*tert*-butylamino-2',6'-dichlorophenyl]-4,4,5,5-tetramethyl-4,5-dihydro-1*H*-imidazol-1-oxyl. Both crystals include zigzag uniform chains made of hydrogen bondings. The magnetism of Cl_2PIMNH is explained by a uniform chain model with $2J_1/k_B$ = –3.4 K and gapless ground state is suggested. On the other hand, the temperature dependence of χ_p in F_2PIMNH shows a maximum at around 3.4 K, and the χ_p values decrease rapidly below this temperature and goes exponentially to zero as $T \to 0$. Singlet ground state of this material is suggested. The magunitude of the energy gap, Δ = 3.1 K, was estimated by fitting the data below 2.4 K with the expression of $\chi \propto \exp(-\Delta/T)$. Comparison of the crystal structure between F_2PIMNH and Cl_2PIMNH, suggests that only F_2PIMNH has significant exchange coupling between the next-nearest-neighbors. The next nearest contact in F_2PIMNH is much shorter than the one in Cl_2PIMNH. There is theoretical expectation for the energy gap in the Heisenberg antiferromagnetic chain with the next-nearest-neighbor interaction. F_2PIMNH studied here is the first example of this model exhibiting an energy gap.

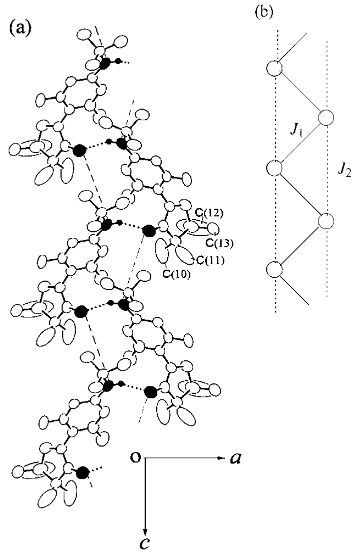

Figure 1. (a) Crystal structure of F_2PIMNH. (b) Scheme of the magnetic interactions in F_2PIMNH.

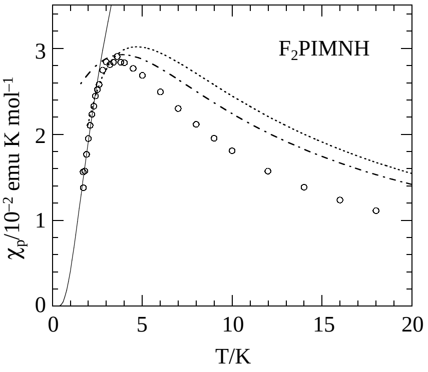

Figure 2. Temperature dependence of χ_p of F_2PIMNH. The solid curve is the fit of $\chi \propto \exp(-\Delta/T)$ with Δ = 3.1 K. The dotted broken curve is the calculation for the uniform chain with $2J/k_B$ = –6 K, the interchain interactions by the mean-field treatment of $2zJ'/k_B$ = -5.2 K are adopted. The dotted curve represents the calculation for the alternating chain with $2J/k_B$ = –7.9 K and $2zJ'/k_B$ = –6.3 K.

V-F-2 Magnetic Properties of Low Dimensional Quantum Spin Systems Made of Stable Organic Biradicals PNNNO, F_2PNNNO and PIMNO

HOSOKOSHI, Yuko; NAKAZAWA, Yasuhiro; INOUE, Katsuya; TAKIZAWA, Kohichi[1]; NAKANO, Hiroki[1]; TAKAHASHI, Minoru[1]; GOTO, Tsuneaki[1]
([1]ISSP, Univ. Tokyo)

[*Phys. Rev. B* **60**, 12924 (1999)]

Stable organic biradical crystals PNNNO, F_2PNNNO and PIMNO of the PNNNO family were synthesized. (PNNNO = 2-[4’-(*N*-*tert*-butyl-*N*-oxyamino)phenyl]-4,4,5,5-tetramethyl-4,5-dihydro-1*H*-imidazol-1-oxyl 3-oxide, F_2PNNNO = 2-[2’,6’,-difluoro-4’-(*N*-*tert*-butyl-*N*-oxyamino)phenyl]-4,4,5,5-tetramethyl-4,5-dihydro-1*H*-imidazol-1-oxyl 3-oxide, PIMNO = 2-[4’-(*N*-*tert*-butyl-*N*-oxyamino)-phenyl]-4,4,5,5-tetramethyl-4,5-dihydro-1*H*-imidazol-1-oxyl.) All the molecules have strong intramolecular ferromagnetic exchange couplings to form $S = 1$ species. Depending on the molecular structure, the magnitude of the exchange coupling varies with $2J/k_B \sim$ 200–700 K. Both crystals of PNNNO and F_2PNNNO include similar chain structure formed by the contacts between the nitronyl nitroxide units. However, the magnetic behaviour is quite different from each other. The difference is attributed to the interchain interactions. Only F_2PNNNO has short contacts between the *N*-*tert*-butyl nitroxides as interchain interactions. The different interchain molecular arrangements are related to the difference in the molecular structure. There are noticeable difference in the dihedral angles between the benzene ring and radical planes owing to the electrostatic repulsion between the fluorine atoms and oxygen atoms on radical units. The interchain interactions in F_2PNNNO dominate the magnetism of this compound. The temperature dependence of the susceptibility suggests the existence of the energy gap above the singlet ground state. Moreover, the magnetization isotherm at low temperature exhibits a plateau at half the value of the saturation magnetization. These properties are quite rare among higher-dimensional spin systems than one-dimensional ones. Our theoretical calculation gives a qualitatively good explanation for the observed results.

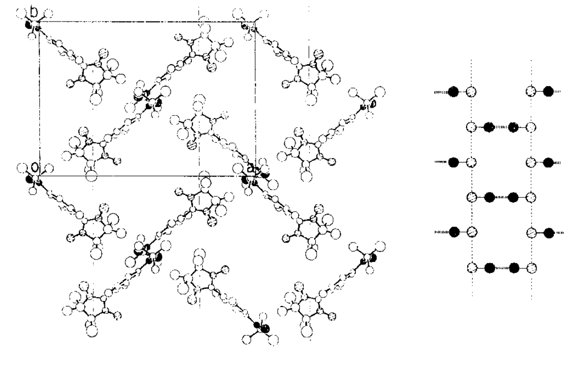

Figure 1. (a) Crystal structure of F_2PNNNO projected on the *ab* plane. *Pbca*, a = 19.857, b = 14.010, c = 13.481 Å, V = 3750.5 Å^3, Z = 8. Black and shaded ellipses represent the *N*-*tert*-butyl nitroxide and nitronyl nitroxide, respectively. (b) Schematic display of the crystal structure of F_2PNNNO. Black and shaded circles are correspond to the *N*-*tert*-butyl nitroxide and nitronyl nitroxide, respectively. Solid and broken lines represent the exchange path of the intra- and intermolecular interactions, respectively.

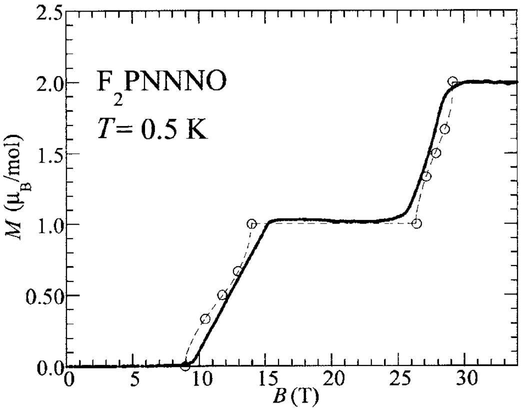

Figure 2. Magnetization process of F_2PNNNO at 0.5 K. Circles represent the calculated results.

V-F-3 Singlet Ground States in an Organic S = 1/2 Spin Ladder and a Novel Double Spin Chain of Ferromagnetic Dimers Formed by an Organic Tetraradical

KATOH, Keiichi; HOSOKOSHI, Yuko; INOUE, Katsuya; GOTO, Tsuneaki[1]
([1]ISSP, Univ. Tokyo)

[*J. Phys. Soc. Jpn.* **69**, 1008 (2000)]

We have synthesized novel organic polyradicals BIP-BNO and BIP-TENO, which crystallize to form spin systems with a double spin chain, where BIP-BNO and BIP-TENO denote 3,5’-bis(*N*-*tert*-butylaminoxyl)-3’,5’-dibromobiphenyl and 3,3’,5,5’-tetrakis(*N*-*tert*-butylaminoxyl)biphenyl, respectively. The crystals of BIP–BNO form a two-leg ladder of S = 1/2 with antiferromagnetic legs and rungs. The ground state of this material is singlet. The BIP–TENO molecule includes S = 1/2 spin pairs (dimers) in which the two spins are coupled ferromagnetically. The BIP-TENO crystals form a double spin chain consisting of dimers. All dimers interact antiferromagnetically with each other. This system can be regarded as an antiferromagnetic two-leg ladder when the dimer is taken as a unit. The ground state of this material is singlet and the existence of excitation gaps is suggested by the temperature dependence of the static magnetic susceptibility.

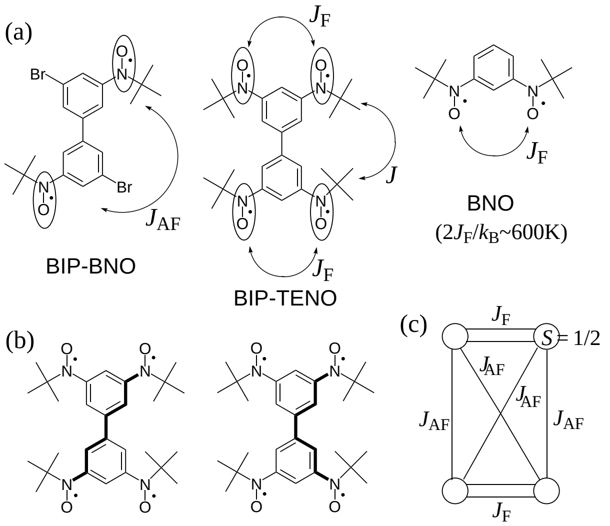

Figure 1. (a) Molecular structures of BIP-BNO, BIP-TENO and a related compound. Ellipses in BIP-BNO and BIP-TENO represent the spin-concentrated parts in a molecule. Each NO group corresponds to an S = 1/2 spin. (b) Path of the throughbond antiferromagnetic exchange interaction in BIP-TENO, which is indicated by bold lines. (c) Schematic diagram of the magnetic model of a BIP-TENO molecule. A circle, a double bond and a single bond represent an S = 1/2 spin, a ferromagnetic exchange coupling, and an antiferromagnetic exchange coupling, respectively.

V-F-4 Observation of Magnetization Plateau of 1/4 in a Novel Double Spin Chain of Ferromagnetic Dimmers Formed by an Organic Tetraradical

GOTO, Tsuneaki[1]; BARTASHEVICH, M. I.[1]; HOSOKOSHI, Yuko; KATOH, Keiichi[2]; INOUE, Katsuya
([1]ISSP, Univ. Tokyo; [2]GUAS)

[*Physica B* in press]

We have measured the susceptibility and low temperature magnetization curve of the novel organic tetraradical crystal BIP-TENO. The susceptibility data indicate that double spin chains of ferromagnetic dimmers are formed in the crystal and the spin system is regarded as an S = 1 antiferromagnetic two-leg ladder. The magnetization is nearly zero up to 10 T and the spin gap is closed at 11.6 T. Above 12 T, the magnetization increases and a plateau corresponding to a quarter of the saturation magnetization appears at 44.8 T.

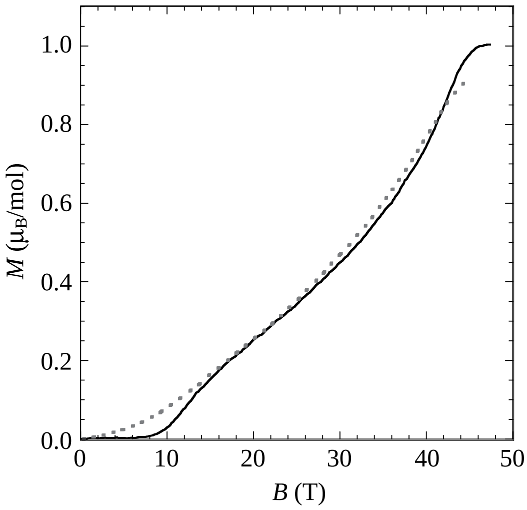

Figure 1. Magnetization curves of BIP–TENO for 1.7 K (solid) and 4.2 K (dotted) in pulsed high magnetic fields up to about 50 T.

V-G Pressure Effects on Molecular Magnetism

'Pressure' is a powerful tool to control the molecular packings and physical properties. The molecule-based materials with small densities are 'soft' and can be expected to exhibit large pressure effects. For the magnetic measurements with high-accuracy, we have developed a small high-pressure clamp cell made of non-magnetic Cu–Ti alloy which can be equipped to a Quantum Design SQUID magnetometer for the dc and ac magnetic measurements. The inner pressure of the clamp cell has been calibrated by the superconducting transition temperature of Pb. We have already discovered that some kind of structural change can be suppressed by pressurization. We are now studying the pressure effects on the molecule-based magnetic materials in wider range. In molecular materials, the spin density are delocalized and distributed in a molecule and the spin-density-distribution plays an important role in the exchange interactions. It is attractive to control the sign of the exchange coupling by pressurization. The pressure effects on the related compounds with similar crystal structures are studied.

V-G-1 Pressure Effect on Mn Complexes of Bisaminoxyl Radicals

HOSOKOSHI, Yuko; SUZUKI, Kentaro[1]; INOUE, Katsuya; IWAMURA, Hiizu[2]
([1]GUAS; [2]Kyushu Univ.)

[*Mol. Cryst. Liq. Cryst.* **334**, 511 (1999)]

The pressure effects on the magnetic properties of one-dimensional Mn(hfac)$_2$ complexes with 1,3-bis(*N*-*tert*-butylaminoxyl)benzene ($\mathbf{1}_H$) and 5-chloro-1,3-bis(*N*-*tert*-butylaminoxyl)benzene ($\mathbf{1}_{Cl}$) have been studied. These complexes have similar chain structures and, due to the weak interchain interactions, undergo three-dimensional magnetic phase transitions at low temperature. At ambient pressure, the former is a metamagnet with T_N = 5.4 K, and the latter is a ferrimagnet with T_C = 4.8 K. The opposite sign of the interchain interactions in these materials is attributed to the different way of packing of the chains. Application of the pressure less than 7 kbar to these materials mainly affects the interchain interactions. The high-temperature behaviour is almost independent of the pressure. In the metamagnetic compound of [Mn(hfac)$_2$]·**1**$_H$, enhancement of the antiferromagnetic interchain interactions by pressurization was observed. The transition temperature becomes higher and the critical field becomes larger with applying pressure. The closer spacing of each chains caused by pressurization, yields larger antiferromagnetic interchain interactions in this compound. On the other hand, the response to the pressure of the ferromagnetic compound of [Mn(hfac)$_2$]·**1**$_{Cl}$ is rather complicated. The transition temperature becomes higher and the antiferromagnetic interchain interactions are induced by pressurization. The interchain exchange coupling in this compound should be sensitive to the relative orientation of the chain structure. The decrease of the ferromagnetic contribution and/or the increase of the antiferromagnetic one in the interchain interactions is brought about by pressurization.

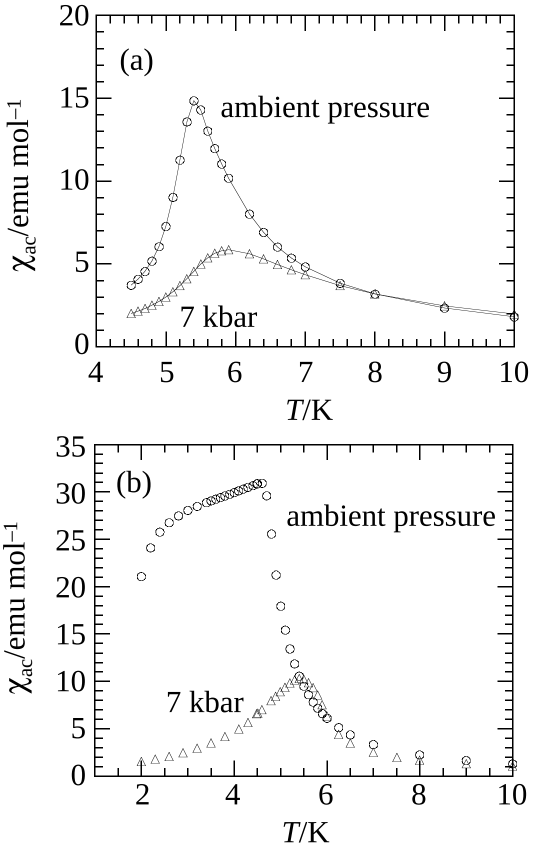

Figure 1. (a) Temperature dependence of the ac susceptibility of [Mn(hfac)$_2$]·**1**$_H$ at ambient pressure (○) and under 7 kbar (△). (b) Temperature dependence of the ac susceptibility of [Mn(hfac)$_2$]·**1**$_{Cl}$ at ambient pressure (○) and under 7 kbar (△).

V-G-2 Pressure Effect on Cu(hfac)$_2$ Complex with 5-Bromo-1,3-phenylenebis(*N-tert*-butyl-aminoxyl)—Suppression of the Structural Change under Pressure

HOSOKOSHI, Yuko; IWAHORI, Fumiyasu[1]**; SUZUKI, Kentaro**[1]**; INOUE, Katsuya**
([1]GUAS)

5-Bromo-1,3-phenylenebis(*N-tert*-butyl-aminoxyl) (**1**) forms a complex with Cu(hfac)$_2$ with the formula [Cu(hfac)$_2$]$_3$·**1**$_2$. The X-ray crystal structural analysis at room temperature revealed the discrete cluster formation of this unit. The temperature dependence of the susceptibility shows abrupt decrease at around 48 K with thermal hysteresis. The structural change at this temperature is suspected. We studied the magnetic properties under pressure and found that the anomaly at around 48 K disappears under 6 kbar. The susceptibility behaviour under 6 kbar is well understood based on the room-temperature crystal structure. Starting from the non-interacting 3 mol of S = 1/2 spin at room temperature, as temperature decreases, ferromagnetic exchange couplings within a cluster dominates the magnetism.

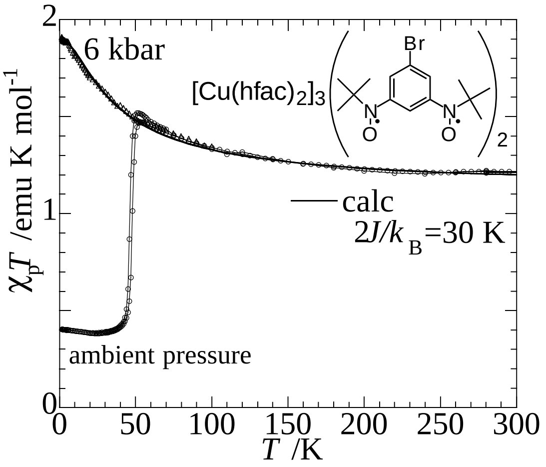

Figure 1. Temperature dependence of $\chi_p T$ of [Cu(hfac)$_2$]$_3$·**1**$_2$ at ambient pressure (○) and under pressure (△). Solid curve is the calclation for the ferromagnetic linear trimer model with $2J/k_B$ = 30 K.